



Study on the characteristics of biochar from Yak Dung in Tibet: focused on adsorption of arsenic and fluoride in geothermal water

Hui Bai^a, Chunhui Luo^b, Dan Ge^c, Duo Bu^c, Zeng Dan^c, Xuebin Lyu^{a,c,*}

^a*School of Environmental Science and Engineering, Tianjin University, Tianjin 300072, China, Tel. +86-22-87402148; email: xbltju@tju.edu.cn (X. Lyu)*

^b*Smart Water Design & Research Institute, North China Municipal Engineering Design & Research Institute Co.,Ltd., Beijing 102600, China, email: luochunhui@tju.edu.cn (C. Luo)*

^c*Department of Chemistry and Environmental Science, School of Science, Tibet University, Lhasa 850000, China, Tel. +183-8902-9086; email: 3320676324@qq.com (D. Ge)*

Received 14 November 2019; Accepted 8 April 2020

ABSTRACT

Arsenic and fluoride are two typical elements found in high concentrations in geothermal water in Tibet. In this study, a series of biochar (BC500, BC600, BC700 and BC800) and modified biochar (Fe-BC600) were prepared from yak dung, a unique biomass resource in Tibet, and used to adsorb As(V) and F⁻ in local geothermal water. The effects of solution pH, temperature, adsorbent dosage and other coexisting ions were studied. The maximum removal rate of As(V) by Fe-BC600 was 98.52% when the adsorbent dosage was 3 g/L, while that of F⁻ was 98.11% when the dosage was 4 g/L at pH = 7 and 80°C. Compared with BC600, the maximum adsorption capacity of Fe-BC600 for As(V) increased six-fold, while the saturated adsorption capacity for F⁻ remained unchanged. In the presence of Ca²⁺, Mg²⁺, Cl⁻, SO₄²⁻ and HCO₃⁻, Fe-BC600 showed no degradation during the removal of As(V) and F⁻ removal, and the removal rates of As(V) and F⁻ decreased minimally, even after five desorption–adsorption cycles. The chemical and physical structures of the biochar were characterized by Brunauer–Emmett–Teller surface area analysis, X-ray diffraction, Fourier-transform infrared spectroscopy, scanning electron microscopy and X-ray fluorescence spectroscopy. We demonstrated that the adsorption kinetics on Fe-BC600 followed the pseudo-second-order model and that the adsorption process was endothermic and spontaneous.

Keywords: Yak dung biochar; Arsenic; Fluoride; Geothermal water; Adsorption; Desorption

1. Introduction

Geothermal water is a clean, natural resource that has been used for power generation, medical treatment, bathing, etc. China's geothermal resources account for about 8% of total geothermal energy reserves on earth, and are mainly distributed in southern Tibet, western Sichuan, western Yunnan and Taiwan [1,2]. However, most of the wastewater generated during power generation and from bathing facilities is discharged without treatment. Fluorine (F) and

arsenic (As) are two harmful elements typically found in high concentrations in geothermal water. According to the World Health Organization (WHO), the upper limit of the concentration of F and As in drinking water is 1.5 and 0.01 mg/L, respectively. Yet, levels in groundwater often exceed these limits. For example, in the Yangbajing shallow geothermal system in Tibet, the concentrations of F and As are 18.9 and 2.99 mg/L, respectively [3]. If geothermal water were to mix with human drinking water sources, it could lead to numerous long-term, deleterious effects on

* Corresponding author.

the local human population health, such as organ failure, keratosis, lung cancer, skin cancer, and skin pigmentation issues [4,5].

The methods for removing As from water are generally classified as either physical, such as flocculation, precipitation and membrane separation; or chemical, such as precipitation [6]. Adsorption, precipitation and membrane separation methods are the main methods for removing fluorine from water [7]. Generally, adsorption is considered to be the most promising technology in wastewater treatment due to its cost-effectiveness and environmental friendliness [8,9].

Biochar is a porous, highly aromatic, water-insoluble solid material formed by carbonizing biomass under anoxic conditions [10–12]. As an adsorbent, it has high stability, large specific surface area, strong adsorption capacity and low-cost; and has already demonstrated excellent capabilities in pollutant adsorption, particularly with Cr, Pb, As, Cu, Cd and F⁻ [13,14]. The adsorption capacity of biochar can also be improved by surface modification. Yang et al. [15] prepared biochar-supported Fe(0) nanoparticles (nZVI-BC) to remove Cd(II) and As(III) from aqueous solution. Takaya et al. [16] demonstrated that modifying biochar with Mg resulted in an increased absorption capacity for phosphate, from a 2.1%–3.6% to 66.4%–70.3%. Zhang et al. [17] loaded Fe onto biochar to adsorb As(V) in water, while Kim et al. [18] modified biochar from *Miscanthus* with amorphous iron (hydr) oxide to completely remove arsenite from aqueous solution. Wendimu et al. [19] modified bamboo biochar with AlCl₃/FeCl₃ to increase the adsorption capacity of F⁻.

Tibet is rich in biomass resources, but yak dung is perhaps the most unique. It is a valuable fuel source for the local population, who uses large quantities for cooking and heating. Yak dung has been previously used to prepare biochar, and further modification with FeCl₂ resulted in an adsorbent that completely removed As and F from geothermal water [20]. In this paper, the preparation method for modified and unmodified biochar from yak dung is refined, and the resulting adsorbents were fully characterized. The effects of pH, temperature, adsorbent dosage and other coexisting ions on As and F removal rate by different biochar were also studied. The adsorption process was described from both kinetics and thermodynamic perspectives, and the regeneration performance was studied using desorption–adsorption cycling. This study seeks to address local environmental problems by using a local biomass resource and provides inspiration and new ideas for dealing with geothermal water pollution in Tibet.

2. Experimental methods and product analysis

2.1. Experimental materials

Yak dung was obtained from a pasture in the plateau area of Eastern Tibet. Fluorine standard solution (1,000 mg/L) was purchased from Tianjin Guangfu Fine Chemical Research Institute, (Tianjin, China) and arsenic standard solution (1,000 mg/L) was purchased from Shanghai ANPEL Experimental Polytron Technologies Inc., (Shanghai, China). Nitric acid (HNO₃) was obtained from Tianjin Jiangtian Chemical Technology Co., Ltd., (Tianjin,

China). Ferrous chloride (FeCl₂) was purchased from Tianjin Guangfu Fine Chemical Research Institute, (Tianjin, China). Sodium hypochlorite (NaClO) was purchased from Tianjin Yuanli Chemical Co., Ltd., (Tianjin, China).

2.2. Synthesis of modified biochar (Fe-BC600)

The yak dung was made into biochar according to a previous method [20]. Yak dung was naturally air-dried, then further dried at 105°C for 2 h. Dried dung was then crushed and passed through a 100 mesh sieve. A certain amount of yak dung was then weighed out and placed into a tube furnace. The tube was purged with nitrogen for 20 min before heating at 500°C, 600°C, 700°C or 800°C for 3 h with a heating ramp rate of 10°C/min. The yak fecal biochar (BC) were labeled according to their respective pyrolysis temperature: BC500, BC600, BC700 and BC800. Biochar samples were then added to 1.0 mol/L HNO₃ at a solid–liquid ratio of 1:25 (m/V, g/ml), washed for 30 min in water, and then the supernatant was carefully removed [21]. Finally, the resulting solid was washed with ultra-pure water until the filtrate was neutral, and the obtained solid was dried at 105°C.

Modified biochar (Fe-BC600) was prepared according to a previously published method [22]. BC600 was added to 0.1 mol/L FeCl₂ solution at a solid–liquid ratio of 1:15 (g/mL) and stirred for 24 h. Sodium hypochlorite solution was then added to the BC600/FeCl₂ mixture every 6 h according to the ratio of $n(\text{FeCl}_2 \cdot 4\text{H}_2\text{O}) : V(\text{NaClO})$ to 0.1 mol:40 mL. The pH of the solution was adjusted to between 4.5 and 5.0 with 1 mol/L HCl and NaOH. After 24 h, the obtained modified biochar was washed and filtered and dried at 80°C.

2.3. Experimental method and product analysis

2.3.1. Influencing factors

2.3.1.1. pH, temperature and adsorbent dosage

A certain amount of biochar was suspended in either 20 mL 4.0 mg/L As(V) solution or 20 mL 19.0 mg/L F⁻ solution, and heat-shocked for 24 h in a constant temperature oscillator. The solution was then filtered through a syringe-driven filter and the concentration of adsorbate was measured in order to calculate the adsorption capacity and removal rates.

2.3.1.2. Other coexisting ions

Ca²⁺ (approx. 4.6 mg/L), Mg²⁺ (approx. 0.3 mg/L), Cl⁻ (approx. 500 mg/L), SO₄²⁻ (approx. 60 mg/L) and HCO₃⁻ (approx. 160 mg/L) were studied as coexisting ions in adsorption studies. The amount of adsorbed As and F⁻, as well as other ions, was calculated as the difference in concentration between the initial and final solution. The mixed solution was prepared according to the concentration of each ion found in natural geothermal water [3,23].

2.3.2. Desorption experiment

Desorption studies were carried out according to a previously published method [24]. 0.2 g Fe-BC600 was placed in a 100 mL Erlenmeyer flask with 50 mL mixed solution

containing 4.0 mg/L arsenic and 19.0 mg/L fluorine. The flask was then heated in a water bath thermostat shaker (25°C) for a certain amount of time. The saturated biochar was then divided and transferred into vials containing different desorbents 20 mL 0.1 mol/L HCl solution, 20 mL 0.1 mol/L NaOH solution or 20 mL methanol. After 5 h, the biochar residue was filtered, washed with ultra-pure water, and dried. They were then used in the repeated adsorption experiments to study the regeneration performance after desorption-adsorption cycles.

2.3.3. Analysis method

As concentrations were determined with an inductively coupled plasma-optical emission spectrometer (ICP-OES, Thermo, 7000 series, United States), and F⁻ concentrations were measured with a fluoride ion meter (Rex Electric Chemical, PXSJ-216, China). All tests were repeated in triplicate.

2.4. Characterization

The specific surface area of the biochar sample was measured with a Brunauer–Emmett–Teller (BET) specific surface area analysis tester (BET A201A, Beijing Guanzheng Precision Electric Instrument Equipment Co., Ltd., China). X-ray diffraction (XRD) (XRD-6100, Shimadzu Enterprise Management Co., Ltd., China) was used to analyze the composition of biochar. The functional groups contained in the biochar were analyzed by Fourier-transform infrared spectroscopy (FTIR) (Cary 660, Agilent Technologies Co., Ltd., USA). The microstructure and morphology of the biochar were analyzed by scanning electron microscopy (SEM) (SIGMA 300, Beijing Oubo Optics Technology Co., Ltd., China). Qualitative and quantitative analysis of the elements contained in the biochar was carried out by X-ray fluorescence (XRF) analysis (EDX1800B, Shenzhen Bairuiyi Technology Co., Ltd., China).

2.5. Kinetics and isotherm analysis

2.5.1. Kinetic

Herein, the adsorption kinetics of As(V) and F⁻ onto BC600 and Fe-BC600 were fitted using quasi-first-order [Eq. (1)] and pseudo-second-order [Eq. (2)] kinetic models:

$$\ln(q_e - q_t) = \ln q_e - k_1 t \quad (1)$$

$$\frac{t}{q_t} = \frac{1}{k_2 q_e^2} + \frac{t}{q_e} \quad (2)$$

where the values of q_e and k_2 were obtained from the intercept and slope of the linear plot of t/q_t vs. t .

2.5.2. Isotherm analysis

The Langmuir [(Eq. (3)), Freundlich [(Eq. (4)), Dubinin–Radushkevich (D–R) [Eqs. (5) and (6)], and Temkin [Eq. (7)] adsorption isotherms were used to fit and compare the two adsorption models for the adsorption data.

$$q_e = \frac{K_L q_m C_e}{K_L C_e + 1} \quad (3)$$

$$q_e = K_F C_e^{\frac{1}{n}} \quad (4)$$

$$\ln q_e = \ln q_m - K_{DR} \varepsilon^2 \quad (5)$$

$$\varepsilon = RT \ln \left(1 + \frac{1}{C_e} \right) \quad (6)$$

$$q_e = \frac{RT}{b_i} \ln a_i + \frac{RT}{b_i} \ln C_e \quad (7)$$

2.6. Adsorption thermodynamic model

Adsorption experiments were carried out at 25°C, 50°C, and 80°C for studying thermodynamics. Standard Gibbs free energy (ΔG°) [Eq. (8)]; and standard enthalpy (ΔH°) and standard entropy (ΔS°) [Eq. (9)] were then calculated and used to describe the reaction process. Thermodynamic parameters were calculated by the following equations:

$$\Delta G = -RT \ln K_b \quad (8)$$

$$\ln K_b = \frac{\Delta S}{R} - \frac{\Delta H}{RT} \quad (9)$$

Using the adsorption amount and concentration at the adsorption equilibrium at different temperatures, the thermodynamic constant K_b was calculated from the linear plot $\ln(q_e/C_e)$ vs. q_e (Figs. 1 and 2), and ΔG was calculated according to Eq. (8). Finally, using Eq. (9), the linear plot of $\ln K_b$ vs. $1/T$ was obtained (Figs. 3 and 4), and ΔH and ΔS were calculated from the slope and intercept respectively.

3. Results and discussion

3.1. Effects of pH, temperature, adsorbent dosage and other coexisting ions on As and F removal rate by different biochars

3.1.1. pH

The removal rate and adsorption amount of As(V) in biochar gradually decreased with increasing pH and the removal rate was lower than 10% at pH 8–9 pH (Fig. 5a). Among BC500 [20], BC600, BC700 and BC800, BC600 removed the most As(V), whereas BC600 and BC700 removed the most F⁻, with removal rates of 97.26% and 98.35% respectively at pH 7 (Fig. 5b). It was concluded that pH 7 was the optimal pH for adsorption studies.

3.1.2. Temperature

The As(V) removal efficiency of Fe-BC600 was higher than that of BC600, where the addition of Fe increased

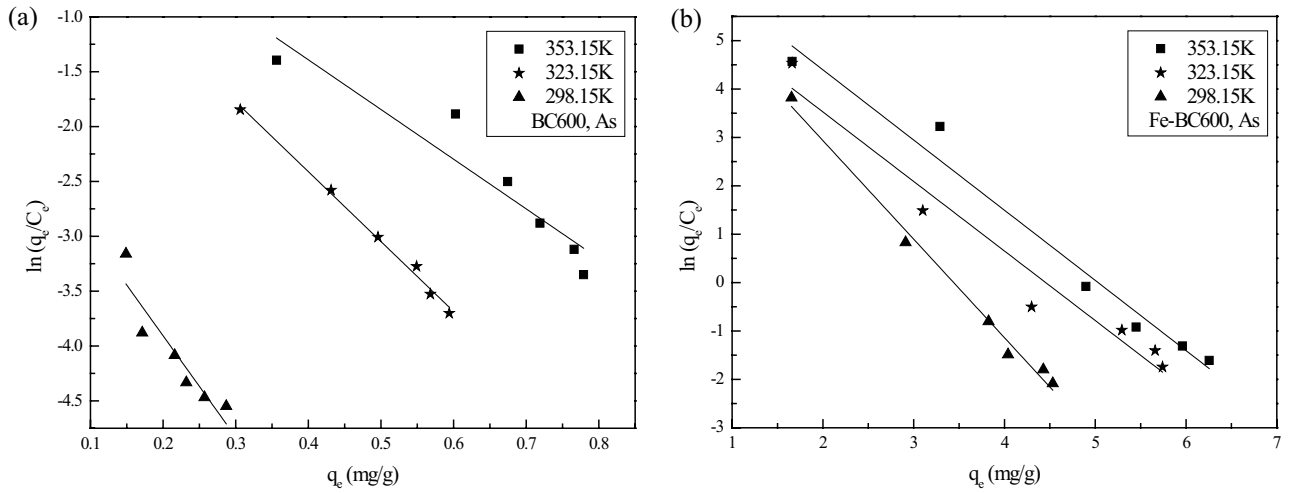


Fig. 1. q_e - $\ln(q_e/C_e)$ fitting curve of (a) BC600 and (b) Fe-BC600 biochar on As(V) at 298.15, 323.15, and 353.15 K.

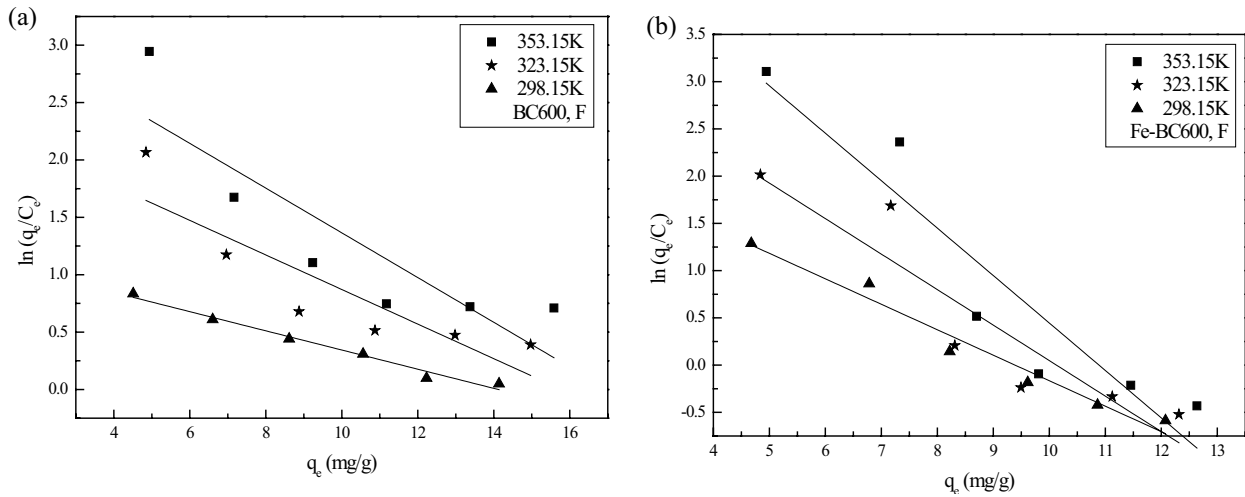


Fig. 2. q_e - $\ln(q_e/C_e)$ fitting curve of (a) BC600 and (b) Fe-BC600 on F^- at 298.15, 323.15, and 353.15 K.

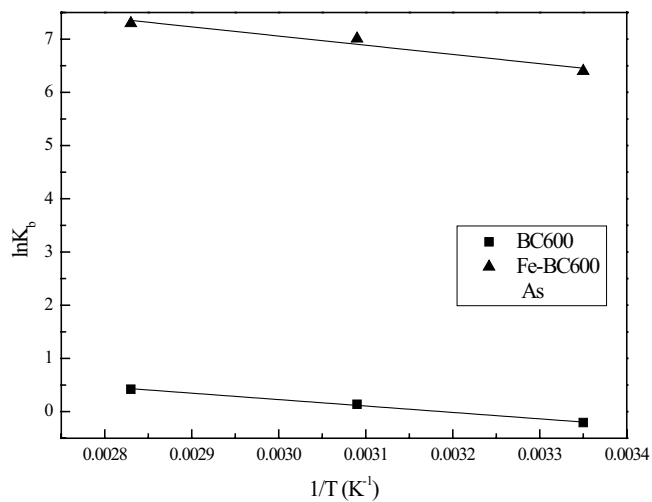


Fig. 3. $1/T$ - $\ln K_b$ fitting curve of BC600 and Fe-BC600 on As(V).

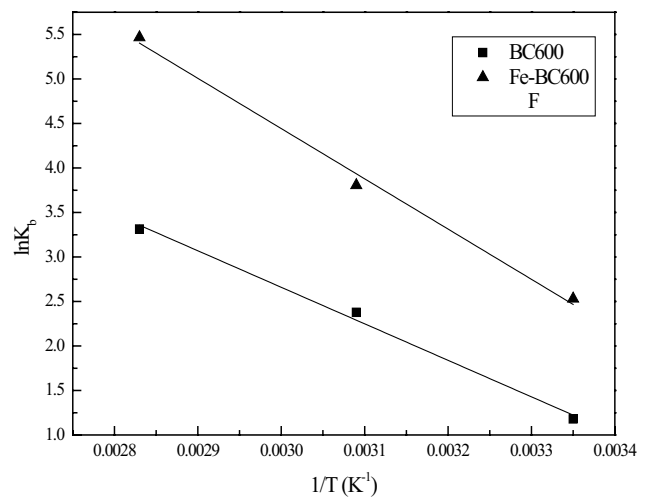


Fig. 4. $1/T$ - $\ln K_b$ fitting curve of BC600 and Fe-BC600 on F^- .

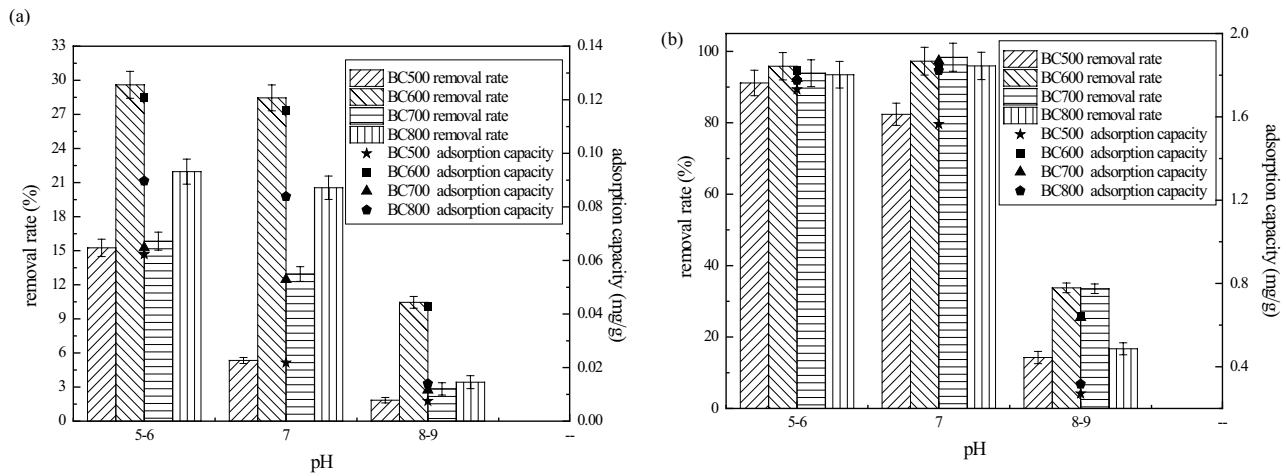


Fig. 5. Removal rates of (a) As(V) and (b) F⁻ under different pH (5–6, 7, 8–9) at 25°C, adsorbent dosage of 10 g/L, by BC500 [20], BC600, BC700, and BC800.

the removal efficiency from approx. 30% to over 99%, and the adsorption capacity increased from 0.10 to 0.40 mg/g (Fig. 6a). The removal rate and adsorption capacity of As(V) from BC600 increased with temperature, while the removal rate of As(V) from Fe-BC600 was unaffected by temperature. Meanwhile, the addition of Fe to the biochar made little impact on its removal efficiency of F⁻, both exhibiting a removal rate of approx. 98% and adsorption capacity of approx. 1.85 mg/g (Fig. 6b). For both BC600 and Fe-BC600, the removal efficiency of F⁻ showed negligible change with increasing temperature.

3.1.3. Adsorbent dosage

The optimal dosage of BC600 was found to be 10 g/L, and the removal rate of As(V) is 64.99%, while the optimal dosage of Fe-BC600 was 3 g/L with a removal rate of 98.52% (Fig. 7a). When the dosage was set 8 g/L for both BC600 and Fe-BC600, the removal rate of As(V) reached as high as

98.77%. When the dosage of BC600 was set between 2 and 4 g/L, the removal rate of F⁻ was higher than above 4 g/L (Fig. 7b). However, when the dosage of Fe-BC600 was set between 1–4 g/L, the removal rate of F⁻ gradually increased with dosage, but no further change was observed above 4 g/L. The optimum dosage for both BC600 and Fe-BC600 was found to be 4 g/L, where Fe-BC600 removed up to 98.11% of F⁻ at this dosage.

3.1.4. Other coexisting ions

When 4 g/L Fe-BC600 was added to a mixed solution of 4.0 mg/L As(V) and 19.0 mg/L F⁻ at pH 7 and 80°C, which are conditions consistent with the individual adsorption experiments described above, no competitive adsorption was observed (Fig. 8). In the presence of either Ca²⁺, Mg²⁺ or Cl⁻, the adsorption of As(V) and F⁻ by Fe-BC600 was unaffected, and the removal rate still exceeded 98%. In the presence of either SO₄²⁻ and HCO₃⁻, the adsorption of As(V) and F⁻ was

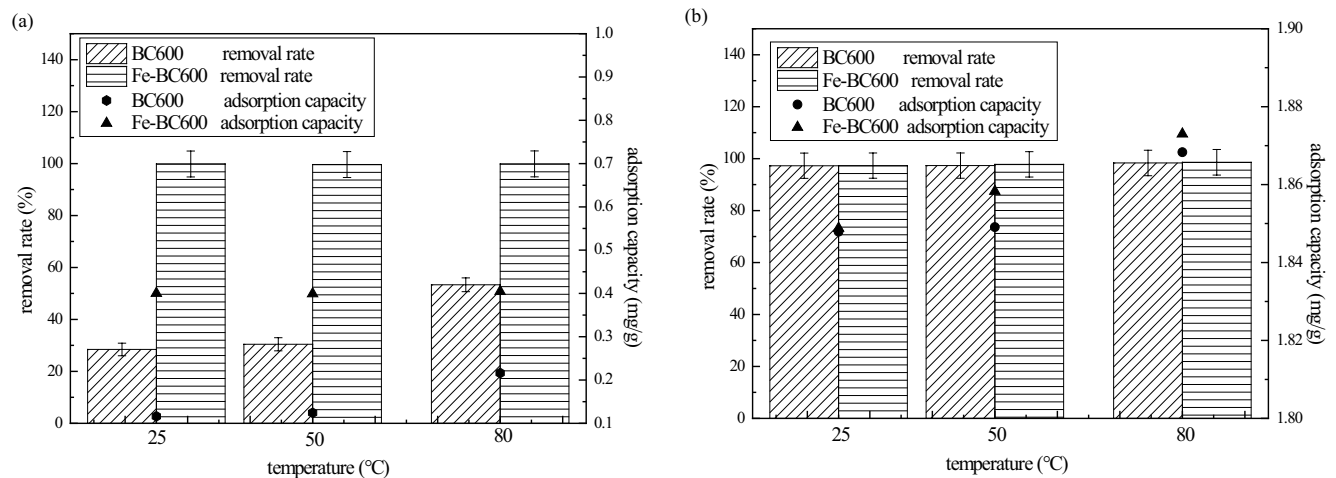


Fig. 6. Removal rates of (a) As(V) and (b) F⁻ at different temperatures (25°C, 50°C, and 80°C) under pH = 7, adsorbent dosage of 10 g/L, by BC600 and Fe-BC600.

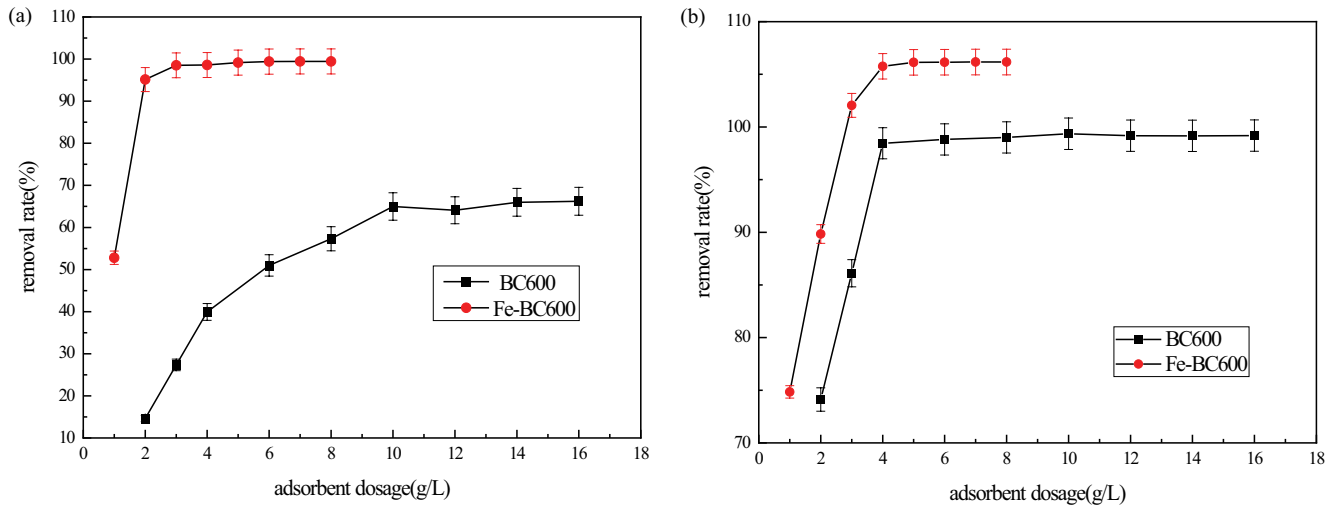


Fig. 7. Removal rates of (a) As(V) and (b) F⁻ at different adsorbent dosages at pH = 7 and 80°C by BC600 and Fe-BC600.

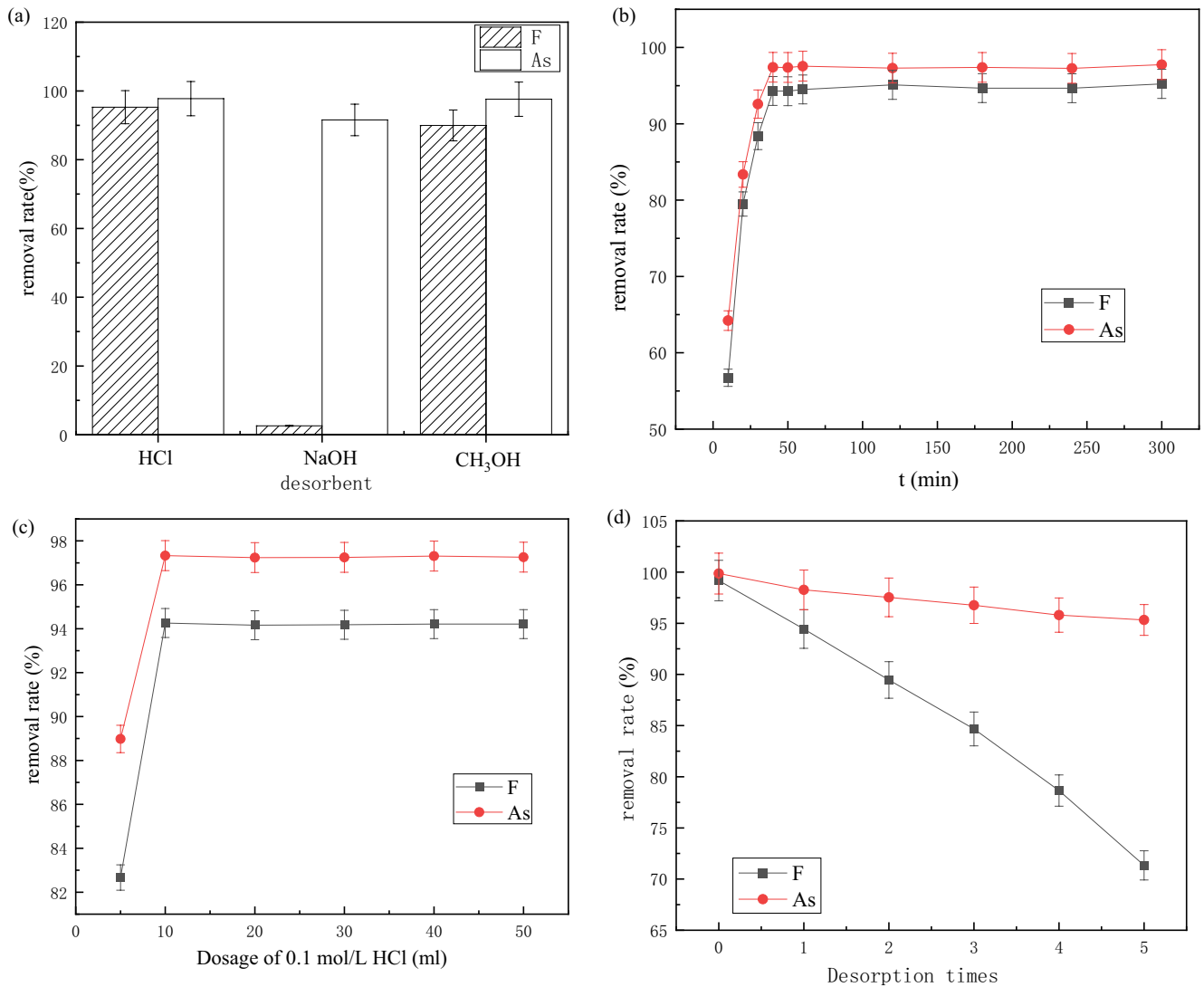


Fig. 8. Removal rates of As(V) and F⁻ by Fe-BC600 in the presence of other ions. The initial concentration of As, F, Ca²⁺, Mg²⁺, Cl⁻, SO₄²⁻ and HCO₃⁻ were 4.0, 19.0, 4.6, 0.3, 500, 60, and 160 mg/L respectively at pH 7 and 80°C with a dosage of 4 g/L of Fe-BC600.

unaffected, but the concentration of SO_4^{2-} and HCO_3^- also decreased, suggesting some competitive adsorption with As(V) and F^- .

3.2. Desorption experiment of Fe-BC600

3.2.1. Selection of desorbents

Desorption was achieved by introducing enriched adsorbents to either concentrated acid (HCl), concentrated base (NaOH) or organic solvent (methanol).

The removal rates of As(V) and F^- from Fe-BC600 in concentration HCl were 99.75% and 96.26%, respectively, which is similar to the initial adsorption rates (Fig. 9a). Meanwhile, the removal rates of As(V) and F^- in concentrated NaOH were 91.56% and 2.58%, respectively; and As(V) and F^- is 99.58% and 89.96%, respectively in

methanol. It was concluded that concentrated HCl was the best desorbent.

3.2.2. Optimal conditions of the desorption process

The optimum desorption time was found to be 40 min, after which 97.41% and 94.30% of As(V) and F^- was removed from Fe-BC600, respectively (Fig. 9b). The optimum dosage of HCl was found to be 10 mL with a concentration of 0.1 mol/L, where any further increase in concentration had little effect on the removal rate (Fig. 9c). Under these conditions, Fe-BC600 exhibited the best removal rates for both As(V) (97.33%) and F^- (94.26%). At longer desorption times, the removal rate of both As(V) (from 99.86% to 95.32%) and F^- (from 99.17% to 71.34%) from Fe-BC600 decreased gradually (Fig. 9d). After five times of desorption-adsorption cycles, Fe-BC600 still had an ideal

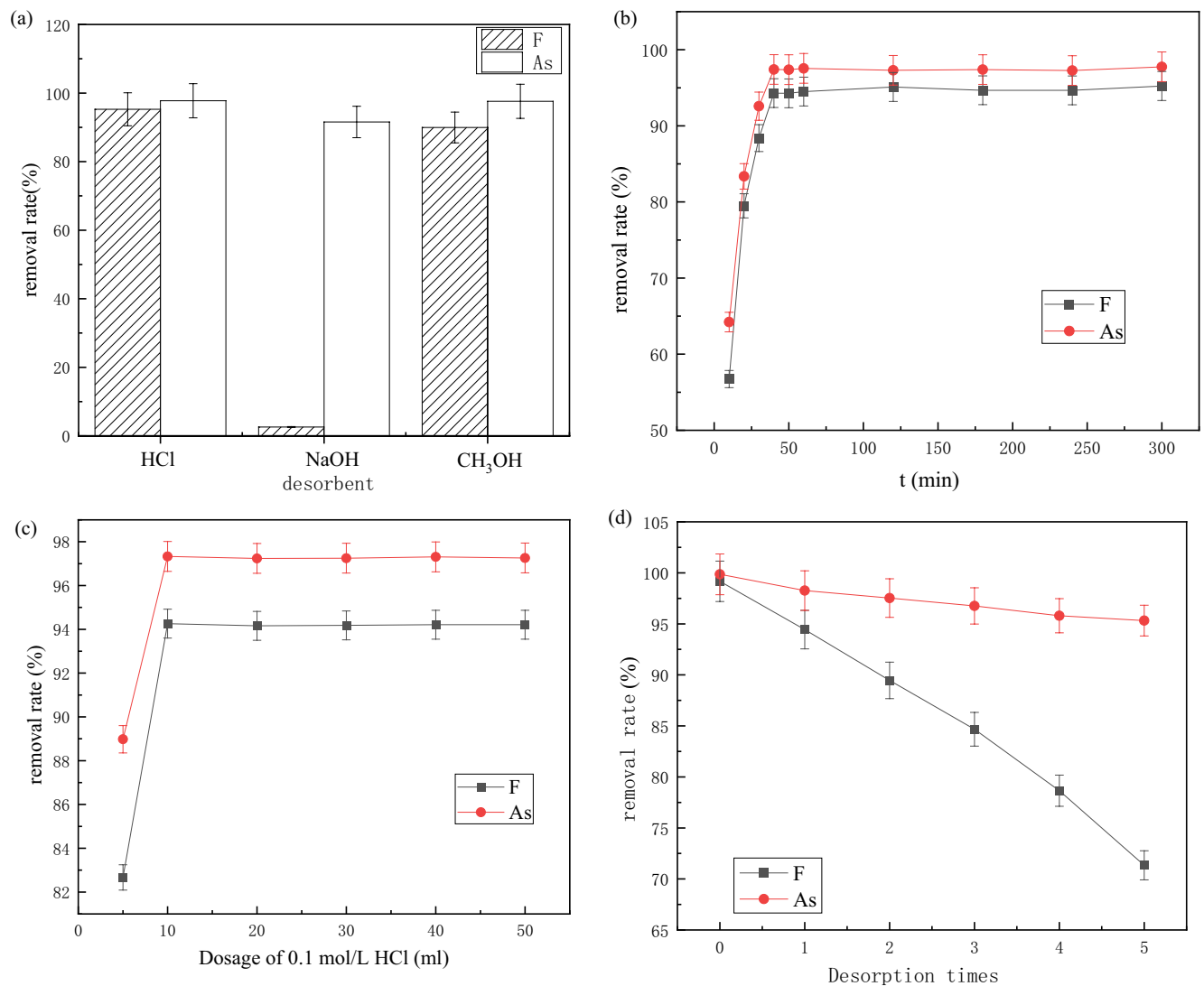


Fig. 9. (a) Removal rates of As(V) and F^- by Fe-BC600 after desorption with different desorbents at pH 7 and 80°C with a dosage of 4 g/L of Fe-BC600, (b) removal rate of As(V) and F^- by 0.2 g Fe-BC600 after desorption in 20 mL 0.1 mol/L HCl at different times, (c) removal efficiency of As(V) and F^- by Fe-BC600 after desorption with different desorbent dosages, and (d) removal efficiency of As(V) and F^- by Fe-BC600 after five successive desorption-adsorption cycles.

adsorption capacity. It was concluded that Fe-BC600 was regenerated with minimal loss of performance, which suggested that it could perform as a cost-effective, recyclable absorbent.

3.3. Biochar characterization

3.3.1. BET analysis

According to BET studies, Fe-BC600 had a smaller specific surface area, pore size and pore volume than BC600 (Table 1), which was due to the back-filling of pores and surfaces with Fe.

Table 1
Specific surface areas, average pore sizes and total pore volumes of BC600 and Fe-BC600

Biochar	Specific surface area (m ² /g)	Average pore size (nm)	Total pore volume (cm ³ /g)
BC600	170.194	26.0159	0.2214
Fe-BC600	155.419	24.6215	0.1913

3.3.2. XRD analysis

XRD analysis showed that modification of the biochar with Fe did not change any constituent crystalline materials, where both patterns show comparable peaks indexed to SiO₂, GaPO₄ and AlPO₄ (Fig. 10a).

3.3.3. FTIR analysis

FTIR spectra for both BC600 and Fe-BC600 had a peak at 3,450–3415 cm⁻¹, assigned to –NH and –OH which are contained in amines, amides, alcohols, phenols, acids and so on (Fig. 10b) [25]. The peak at 2,400 cm⁻¹ was

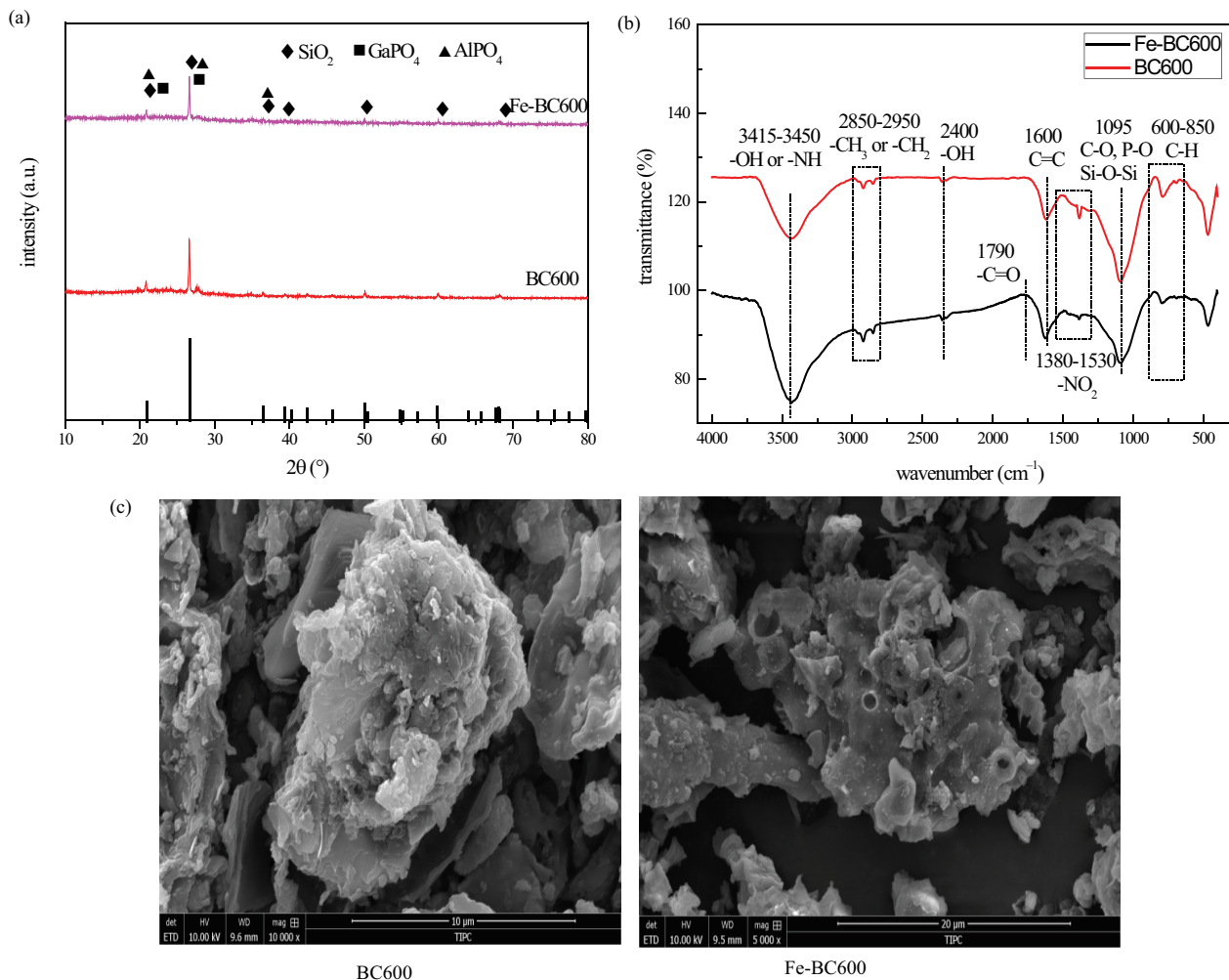


Fig. 10. (a) XRD analysis of BC600 and Fe-BC600, (b) FTIR spectra of BC600 and Fe-BC600, and (c) SEM micrographs of BC600 and Fe-BC600.

assigned to the vibration mode of acid –OH, and the peak at 1,600 cm^{-1} was assigned to aromatic C=C bonds. Yak dung is known to contain large quantities of aromatic moieties that are formed during pyrolysis, but many are also retained from lignin, a major constituent of yak dung [20]. The peak at 1,100 and 1,000 cm^{-1} was assigned to Si–O–Si, but vibrations of P–O and C–O bonds may also contribute [26]. Fe-BC600 yielded a stronger peak than BC600 at Fe-BC600, which suggested the formation of a compound with either stronger bonds, or more numerous bonds. Only Fe-BC600 yielded a peak at 1,790 cm^{-1} which was assigned to a –C=O bond. This was attributed to the introduction of Fe^{2+} during the preparation of the modified biochar, but also their subsequent oxidation to Fe^{3+} , which could yield new acidic oxygen-containing functional groups on the surface of the biochar.

3.3.4. SEM analysis

SEM analysis showed that the surface morphology of Fe-BC600 was smoother than that of BC600 (Fig. 10c). However, the number of micropores on the surface of Fe-BC600 was noticeably lower, which agreed with the lower specific surface area determined by BET analysis. The surface of Fe-BC600 was evenly coated with particles, which were concluded to be Fe-rich compounds supported on the biochar surface. This also confirmed the successful loading of ions onto biochar surfaces.

3.3.5. XRF analysis

Fe-BC600 had a lower oxygen content and a larger proportion of other elements, especially Fe and Cl, than BC600. This demonstrated that Fe was successfully loaded onto biochar.

3.4. Adsorption kinetics and isotherm

3.4.1. Adsorption kinetics

According to experimental adsorption studies, the removal rate of As(V) from solution by BC600 reached equilibrium after approx. 300 min (Fig. 11a), while Fe-BC600 reached equilibrium after approx. 40 min, which was approx. seven-fold faster (Fig. 11b). Adsorption experiments showed that the modification of biochar with Fe also increased the equilibrium adsorption capacity approx. six-fold.

Meanwhile, the adsorption rates and capacity of Fe-BC600 for F^- decreased slightly compared with those of BC600, which was attributed to the lower specific surface area and pore volume after modification.

The fitting parameters and the maximum adsorption amount of the quasi-first-order kinetic and the pseudo-second-order kinetic equation are shown in Table 3. It was shown that the quasi-first-order kinetics and pseudo-second-order kinetics equations best described the adsorption of As(V) and F^- by BC600. The equilibrium adsorption capacity ($q_{e,\text{calc.}}$) was close to the experimental value ($q_{e,\text{exp.}}$), indicating that the adsorption process had both chemical and physical characteristics. Meanwhile,

Table 2
Elemental analysis of BC600 and Fe-BC600

Biochar	BC600	Fe-BC600
O	79.146	65.727
Na	0.445	0.502
Mg	1.086	1.233
Al	1.704	2.001
Si	14.222	18.607
P	0.227	0.317
S	0.376	0.572
Cl	0.035	4.045
K	0.780	1.168
Ca	1.520	2.519
Ti	0.072	0.126
Fe	0.375	3.182
Zr	0.012	–

“–” means not detected

pseudo-second-order kinetics best described the adsorption by Fe-BC600. Since both $q_{e,\text{calc.}}$ and $q_{e,\text{exp.}}$ were closer in value to each other, it was concluded that chemical adsorption was more dominant with Fe-BC600.

3.4.2. Isotherm

Experimental data were then fitted using the Langmuir, Freundlich, D–R and Temkin isotherms (Figs. 12–14 and Table 4). According to the correlation coefficients (R^2) of isotherms of BC600 at different temperatures, the adsorption process was best fitted by the Freundlich isotherm. From this, N was calculated to be greater than 2, which suggested that adsorption became easier as temperature increased. In contrast, the adsorption process of Fe-BC600 was best fitted by the Freundlich and Temkin isotherms. The maximum adsorption capacity (q_{max}) of Fe-BC600 was shown to increase with temperature; and because the calculated value for $1/n$ was smaller, it suggested that Fe-BC600 was better at adsorbing As(V) than BC600.

3.5. Adsorption thermodynamics analysis

The adsorption enthalpies of As(V) on BC-600 and Fe-BC600 were calculated as 10.028 and 14.361 kJ/mol, respectively; while the adsorption enthalpies of F^- on BC-600 and Fe-BC600 were calculated as 34.114 and 46.942 kJ/mol, respectively (Table 5). This suggested that adsorption was endothermic. Calculated ΔG was shown to decrease gradually as the temperature increased, which suggested a stronger spontaneity of adsorption with increasing temperature. Since ΔS was calculated to be greater than zero, it was suggested that the structure of the adsorbent changed during adsorption. This caused an increase in the degree of freedom of the solid–liquid interface, and in turn an increasing degree of disorder of the system [27].

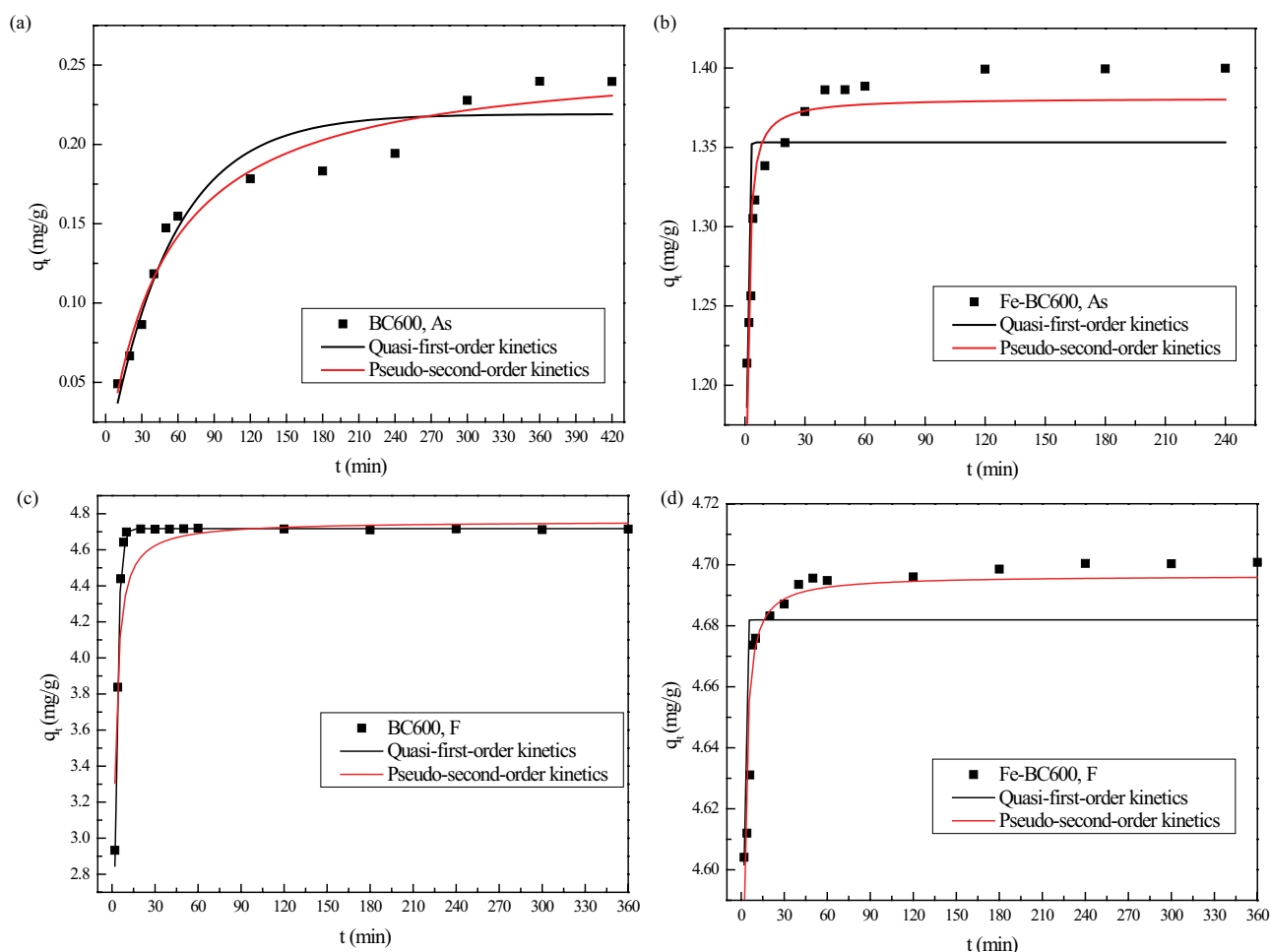


Fig. 11. (a) Quasi-first-order kinetics of As(V) on BC-600, at pH 7 and 80°C; with an initial concentration 4.0 mg/L and adsorbent dosage of 10 g/L. (b) Pseudo-second-order kinetics of As(V) on Fe-BC600, at pH 7 and 80°C; with an initial concentration of 4.0 mg/L; and an adsorbent dosage of 3 g/L. (c) Quasi-first-order kinetics and (d) pseudo-second-order kinetics of F⁻ on BC600 and Fe-BC600 at pH 7 and 80°C; with an initial concentration of 19.0 mg/L and adsorbent dosage of 4 g/L.

Table 3
Quasi-first-order kinetics and pseudo-second-order kinetics fitting parameters for BC600 and Fe-BC600 adsorption

As(V)	Biochar	$q_{e,exp.}$ (mg/g)	Quasi-first-order kinetics			Pseudo-second-order kinetics		
			k_1 (min ⁻¹)	$q_{e,calc.}$ (mg/g)	R^2	k_2 (mg/g min)	$q_{e,calc.}$ (mg/g)	R^2
	BC600	0.2398	0.0186	0.2191	0.9302	0.0798	0.2575	0.9593
	Fe-BC600	1.3999	2.0930	1.3531	0.3408	3.9736	1.3812	0.8475
F ⁻	Biochar	$q_{e,exp.}$ (mg/g)	Quasi-first-order kinetics			Pseudo-second-order kinetics		
			k_1 (min ⁻¹)	$q_{e,calc.}$ (mg/g)	R^2	k_2 (mg/g min)	$q_{e,calc.}$ (mg/g)	R^2
	BC600	4.7196	0.4622	4.7170	0.9908	0.2389	4.7589	0.8335
	Fe-BC600	4.7005	2.0332	4.6819	0.3336	4.3071	4.6965	0.8542

4. Conclusion

This study showed that the modification of biochar with Fe improved the adsorption capacity for As(V), but no significant change was observed for F⁻. Under the experimentally determined optimal adsorption conditions, the removal rates

of As(V) and F⁻ on Fe-BC600 were 98.52% and 98.11%, respectively. The adsorption of As(V) and F⁻ on Fe-BC600 followed the pseudo-second-order kinetic model, while Freundlich models showed a strong fit to the adsorption isotherms of As(V) and F⁻. Desorption-absorption cycles showed that

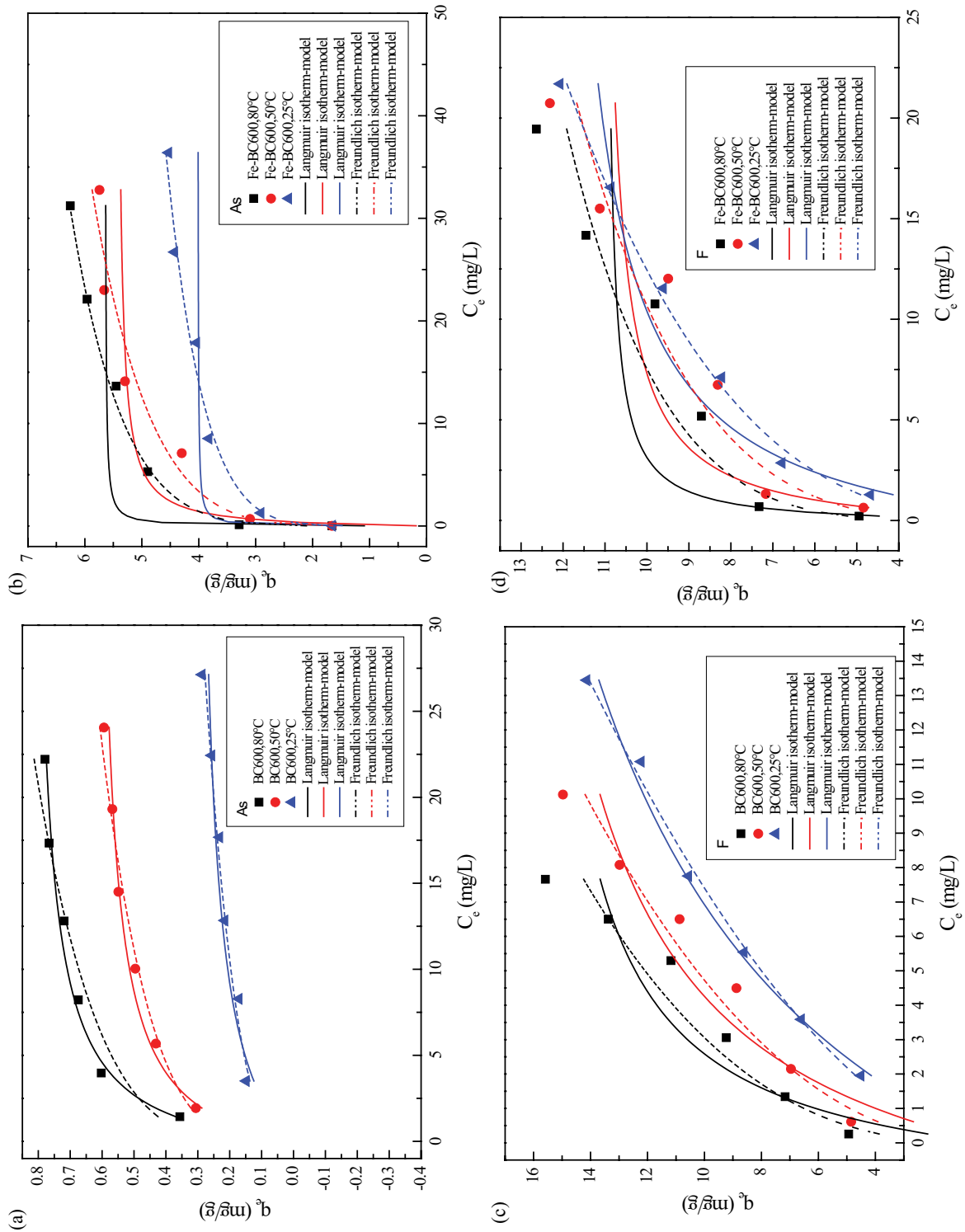


Fig. 12. Freundlich isotherm-model and Langmuir isotherm-model fit for adsorption of As(V) on (a) BC600 and (b) Fe-BC600; and that of F⁻ on (c) BC600 and (d) Fe-BC600.

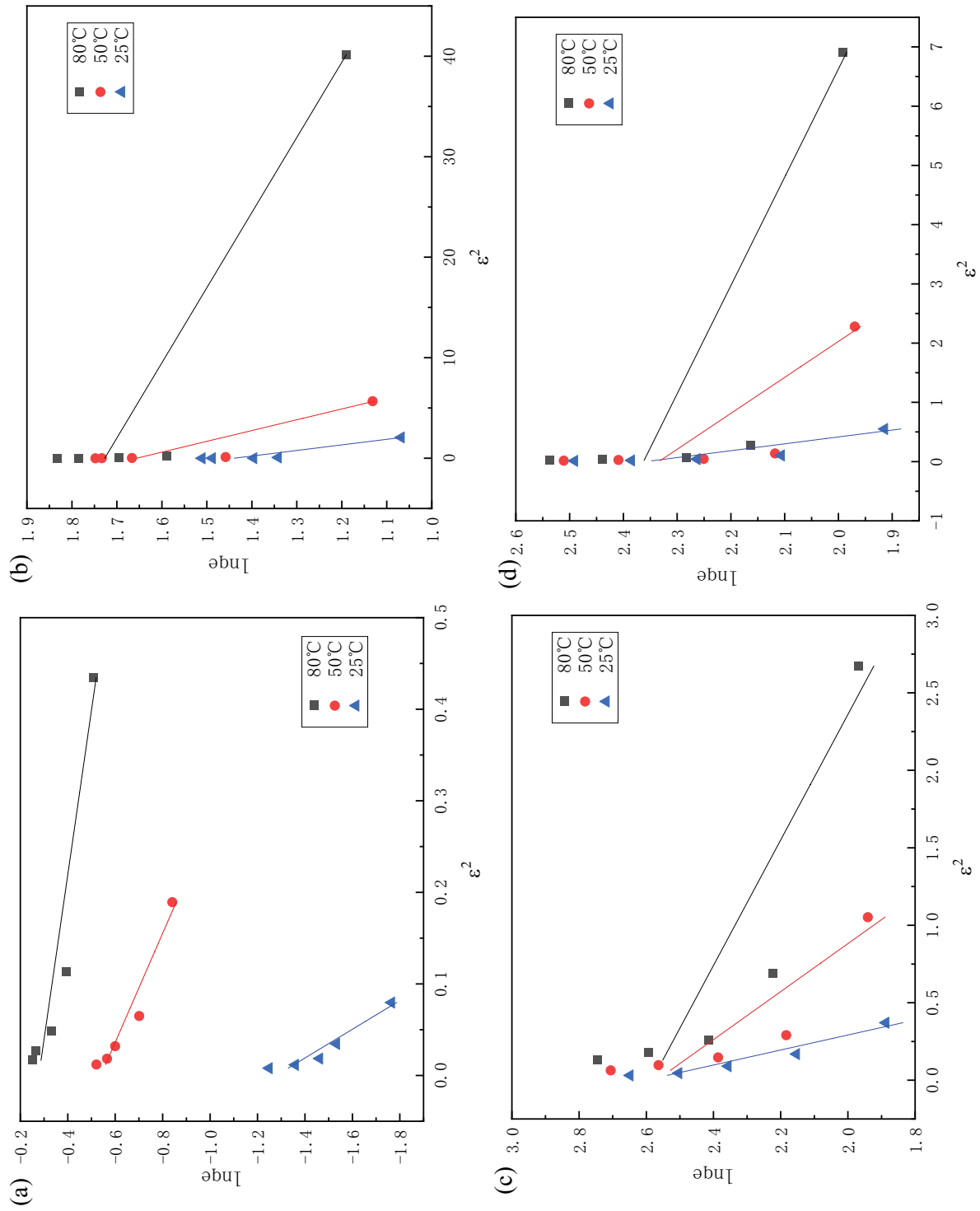


Fig. 13. D–R isotherm-model fits for adsorption of As(V) on (a) BC600 and (b) Fe-BC600; and that of F- on (c) BC600 and (d) Fe-BC600.

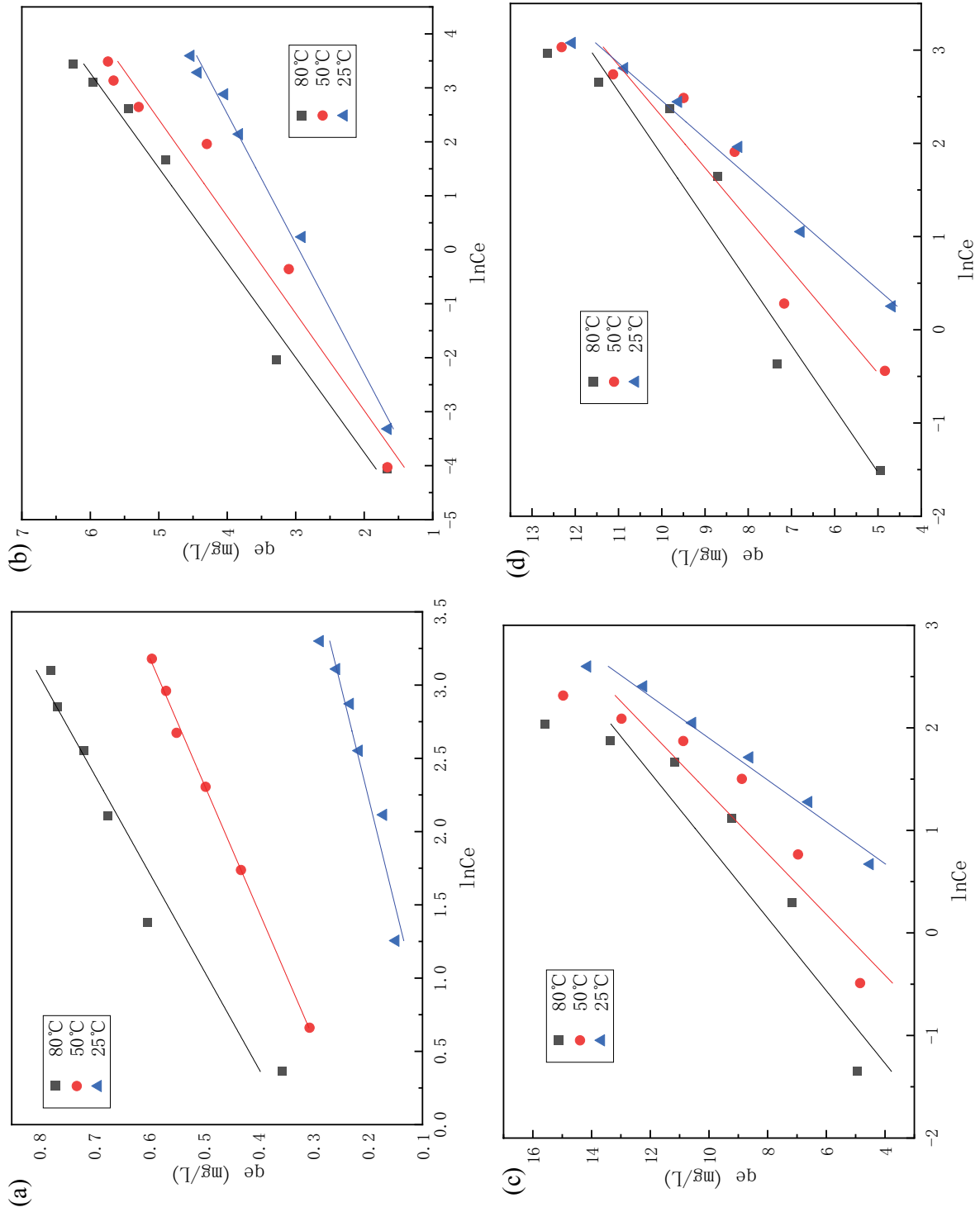


Fig. 14. Temkin isotherm-model fits for adsorption of As(V) on (a) BC600 and (b) Fe-BC600; and that of F- on (c) BC600 and (d) Fe-BC600.

Table 4
Adsorption isotherm data of biochar adsorption

	Biochar	T (°C)	Langmuir			Freundlich		
			q_m	K_L (L/mg)	R^2	K_F (mg/g)	n (g/L)	R^2
As(V)	BC600	80	0.8383	0.5501	0.9860	0.3899	4.2181	0.8915
		50	0.6342	0.4274	0.9721	0.2725	3.9744	0.9820
		25	0.3203	0.1808	0.8439	0.0888	2.8977	0.9567
	Fe-BC600	80	5.6463	13.9581	0.8867	3.8024	6.8966	0.9662
		50	5.4531	1.9547	0.7136	3.2569	5.9195	0.9878
		25	4.0174	16.1377	0.7208	2.7566	7.0934	0.9934
F ⁻	BC600	80	16.7935	0.5696	0.7505	6.5036	2.5968	0.9208
		50	18.6226	0.2725	0.8346	4.8987	2.1760	0.9507
		25	22.5937	0.1147	0.9897	3.1998	1.7567	0.9948
	Fe-BC600	80	11.0397	3.0755	0.7594	6.8949	5.4267	0.9168
		50	11.2172	1.1264	0.7834	5.7647	4.2981	0.9084
		25	12.5026	0.3842	0.9190	4.5361	3.1884	0.9876
	Biochar	T (°C)	D–R			Temkin		
			K_{DR}	E (L/mg)	R^2	b_t (mg/g)	a_t (g/L)	R^2
As(V)	BC600	80	0.5565	0.9479	0.8703	5.0904×10^{-5}	9.8490	0.9549
		50	1.6795	0.5456	0.9298	4.2849×10^{-5}	7.4568	0.9980
		25	6.3714	0.2801	0.9184	2.6662×10^{-5}	2.1699	0.9247
	Fe-BC600	80	0.0134	6.1130	0.8716	1.9380×10^{-4}	1,439.2291	0.9861
		50	0.0931	2.3174	0.8166	2.0708×10^{-4}	716.0811	0.9622
		25	0.1804	1.6648	0.8692	1.6765×10^{-4}	1,220.6361	0.9903
F ⁻	BC600	80	0.2466	1.4240	0.7584	9.6194×10^{-4}	14.6957	0.8491
		50	0.6460	0.8798	0.7709	1.2549×10^{-3}	4.9475	0.8756
		25	2.0630	0.4923	0.9202	1.9774×10^{-3}	1.1511	0.9810
	Fe-BC600	80	0.0547	3.0236	0.5921	5.0036×10^{-4}	138.5809	0.9144
		50	0.1647	1.7425	0.5677	6.7587×10^{-4}	25.0044	0.9057
		25	0.8611	0.7620	0.7469	9.9594×10^{-4}	4.9195	0.9780

Table 5
Thermodynamic parameters of adsorption of As(V) and F⁻ by BC600 and Fe-BC600

	Biochar	T (K)	$\ln K_b$	ΔG (kJ/mol)	ΔH (kJ/mol)	ΔS (kJ/mol K)
As(V)	BC600	298.15	-2.0607×10^{-3}	-5.108	10.028	0.032
		323.15	0.1379×10^{-3}	-0.370		
		353.15	0.421×10^{-3}	-1.236		
	Fe-BC600	298.15	6.4002×10^{-3}	-17.195		
		323.15	7.0074×10^{-3}	-17.370		
		353.15	7.2984×10^{-3}	-21.429		
F ⁻	BC600	298.15	1.1796×10^{-3}	-2.924	34.114	0.124
		323.15	2.3772×10^{-3}	-6.387		
		353.15	3.3133×10^{-3}	-9.728		
	Fe-BC600	298.15	2.5315×10^{-3}	-6.275		
		323.15	3.8052×10^{-3}	-10.223		
		353.15	5.4675×10^{-3}	-16.053		

Fe-BC600 was easily regenerated, and retained excellent adsorption characteristics. We concluded that Fe-BC600 is a promising cost-effective, environmentally friendly adsorbent for the removal of As(V) and F⁻ from geothermal water in Tibet.

Acknowledgements

Hui Bai and Chunhui Luo carried out the lab work, participated in data analysis and drafted the manuscript; Zeng Dan participated in the revision of the manuscript; Dan Ge and Duo Bu collected field data; Xuebin Lyu conceived of the study, designed the study, coordinated the study and helped draft the manuscript.

Funding

This work was supported by Tibet University 2019 Central Financial Support Special Funds for Local Colleges and Universities ([2019] No. 19); Cultivation Foundation of Tibet University (ZDTSJH18-04); the Seed Foundation of Tianjin University (2018XZC-0059).

Symbols

q_e	— Theoretical value for adsorption capacity, mg/g
q_t	— Amount adsorbed at time t , mg/g
k_1	— First-order reaction rate constant, min ⁻¹
t	— Reaction time, min
k_2	— Rate constant of the pseudo-second-order model, mg/g min
q_m	— Maximum adsorption capacity, mg/g
C_e	— Concentration of As(V) or F ⁻ at equilibrium, mg/L
K_L	— Equilibrium constant of Langmuir, L/mg
K_F	— Isothermal constant regarding the adsorption capacity of Freundlich, mg/g
n	— Freundlich isotherm constant, L/g
R	— Ideal gas constant
T	— Temperature, K
K_b	— Thermodynamic equilibrium constant
ΔG	— Gibbs free energy change, kJ/mol
ΔH	— Gibbs metamorphosis, kJ/mol
ΔS	— Gibbs entropy change, kJ/mol K
K_{DR}	— D–R isotherm constant, mol ² /kJ ²
E	— Average adsorption energy, kJ/mol
b_t	— Temkin isotherm constant
a_t	— Temkin isotherm constant

References

- Z.H. Pang, S.P. Huang, S.B. Hu, P. Zhao, L. He, Geothermal studies in China: progress and prospects 1995–2014, *Chin. J. Geol.*, 49 (2014) 719–727.
- L. Zhang, S. Chen, C. Zhang, Geothermal power generation in China: status and prospects, *Energy Sci. Eng.*, 7 (2019) 1428–1450.
- Q.H. Guo, Hydrogeochemistry of high-temperature geothermal systems in China: a review, *Appl. Geochem.*, 27 (2012) 1887–1898.
- Q. Zhang, H. Tan, T. Qu, W. Zhang, Y. Zhang, N. Kong, Impacts of typical harmful elements in geothermal water on river water quality in Tibet, *J. Water Resour. Prot.*, 30 (2014) 23–29.
- T. Tuutijärvi, J. Lu, M. Sillanpää, G. Chen, As(V) adsorption on maghemite nanoparticles, *J. Hazard. Mater.*, 166 (2009) 1415–1420.
- A. Bhatnagar, E. Kumar, M. Sillanpää, Fluoride removal from water by adsorption—a review, *Chem. Eng. J.*, 171 (2011) 811–840.
- R.T. Rao, N.T. Manjunath, Removal of fluoride from aqueous solutions by precipitation, *Eng. Technol.*, 4 (2013) 40–42.
- M. Cledon, R. Galvez, J.R. Vega-Baudrit, Using vegetal biomass for pollution adsorption. Integrated and sustainable environmental remediation, *Am. Chem. Soc.*, 1302 (2018) 1–13.
- M. Hassan, R. Naidu, J.H. Du, Y.J. Liu, F.J. Qi, Critical review of magnetic biosorbents: their preparation, application, and regeneration for wastewater treatment, *Sci. Total Environ.*, 702 (2020) 134893.
- D. Kolodyńska, R. Wnętrzak, J.J. Leahy, M.H.B. Hayes, W. Kwapiński, Z. Hubicki, Kinetic and adsorptive characterization of biochar in metal ions removal, *Chem. Eng. J.*, 197 (2012) 295–305.
- J. Lehmann, J. Gaunt, M. Rondon, Bio-char sequestration in terrestrial ecosystems – a review, *Nat. Commun.*, 11 (2006) 403–427.
- D. Woolf, J.E. Amonette, F.A. Street-Perrott, J. Lehmann, S. Joseph, Sustainable biochar to mitigate global climate change, *Nat. Commun.*, 1 (2010) 56.
- J.S. Clemente, S. Beauchemin, T. MacKinnon, J. Martin, C.T. Johnston, B. Joern, Initial biochar properties related to the removal of As, Se, Pb, Cd, Cu, Ni, and Zn from an acidic suspension, *Chemosphere*, 170 (2017) 216–224.
- J.C. Tang, W.Y. Zhu, R. Kookana, A. Katayama, Characteristics of biochar and its application in remediation of contaminated soil, *J. Biosci. Bioeng.*, 116 (2013) 653–659.
- D. Yang, L. Wang, Z.T. Li, X.J. Tang, M.J. He, S.Y. Yang, X.M. Liu, J.M. Xu, Simultaneous adsorption of Cd(II) and As(III) by a novel biochar-supported nanoscale zero-valent iron in aqueous systems, *Sci. Total Environ.*, 708 (2020) 134823.
- C.A. Takaya, L.A. Fletcher, S. Singh, U.C. Okwuosa, A.B. Ross, Recovery of phosphate with chemically modified biochars, *J. Environ. Chem. Eng.*, 4 (2016) 1156–1165.
- F. Zhang, X. Wang, J. Xionghui, L.J. Ma, Efficient arsenate removal by magnetite-modified water hyacinth biochar, *Environ. Pollut.*, 216 (2016) 575–583.
- J.W. Kim, J.Y. Song, S.-M. Lee, J.H. Jung, Application of iron-modified biochar for arsenite removal and toxicity reduction, *J. Ind. Eng. Chem.*, 80 (2019) 17–22.
- G. Wendimu, F. Zewge, E. Mulugeta, Aluminium-iron-amended activated bamboo charcoal (AIAABC) for fluoride removal from aqueous solutions, *J. Water Process Eng.*, 16 (2017) 123–131.
- C.H. Luo, J. Tian, P.L. Zhu, Z. Bin, D. Bu, X.B. Lu, Simultaneous removal of fluoride and arsenic in geothermal water in Tibet using modified yak dung biochar as an adsorbent, *R. Soc. Open Sci.*, 5 (2018), <https://doi.org/10.1098/rsos.181266>.
- Z.H. Wang, H.Y. Guo, F. Shen, D.Q. Duan, Production of biochar by vermicompost carbonization and its adsorption to Rhodamine-B, *Acta Sci. Circumstant.*, 35 (2015) 3170–3177.
- Y.Y. Du, X. Wang, W.C. Xie, Y. Xiao, X. Wang, X.Y. He, Effects of Fe-impregnated biochar on arsenic immobilization in realgar mine tailings, *Res. Environ. Sci.*, 30 (2017) 159–165.
- Q.H. Guo, Y.X. Wang, W. Liu, Major hydrogeochemical processes in the two reservoirs of the Yangbajing geothermal field, Tibet, China, *J. Volcanol. Geotherm. Res.*, 166 (2007) 255–268.
- F.Z. Khelaifia, S. Hazourli, S. Nouacer, H. Rahima, M. Ziati, Valorization of raw biomaterial waste-date stones-for Cr(VI) adsorption in aqueous solution: thermodynamics, kinetics and regeneration studies, *Int. Biodeterior. Biodegrad.*, 114 (2016) 76–86.
- M. de Godoi Pereira, M. Korn, B.B. Santos, M.G. Ramos, Vermicompost for tinted organic cationic dyes retention, *Water Air Soil Pollut.*, 200 (2009) 227–235.
- J. Meng, X.L. Feng, Z.M. Dai, X.M. Liu, J.J. Wu, J.M. Xu, Adsorption characteristics of Cu(II) from aqueous solution onto biochar derived from swine manure, *Environ. Sci. Pollut. Res.*, 21 (2014) 7035–7046.
- S.-Y. Yoon, C.-G. Lee, J.-A. Park, J.-H. Kim, S.-B. Kim, S.-H. Lee, J.-W. Choi, Kinetic, equilibrium and thermodynamic studies for phosphate adsorption to magnetic iron oxide nanoparticles, *Chem. Eng. J.*, 236 (2014) 341–347.